

Search for the Flavor Changing Neutral Current Decay $t \rightarrow Zq$
in $p\bar{p}$ Collisions at $\sqrt{s} = 1.96$ TeV

T. Aaltonen,²⁴ J. Adelman,¹⁴ T. Akimoto,⁵⁶ M.G. Albrow,¹⁸ B. Álvarez González,¹² S. Amerio^u,⁴⁴ D. Amidei,³⁵
A. Anastassov,³⁹ A. Annovi,²⁰ J. Antos,¹⁵ G. Apollinari,¹⁸ A. Apresyan,⁴⁹ T. Arisawa,⁵⁸ A. Artikov,¹⁶
W. Ashmanskas,¹⁸ A. Attal,⁴ A. Aurisano,⁵⁴ F. Azfar,⁴³ P. Azzurri^s,⁴⁷ W. Badgett,¹⁸ A. Barbaro-Galtieri,²⁹
V.E. Barnes,⁴⁹ B.A. Barnett,²⁶ V. Bartsch,³¹ G. Bauer,³³ P.-H. Beauchemin,³⁴ F. Bedeschi,⁴⁷ P. Bednar,¹⁵
D. Beecher,³¹ S. Behari,²⁶ G. Bellettini^q,⁴⁷ J. Bellinger,⁶⁰ D. Benjamin,¹⁷ A. Beretvas,¹⁸ J. Beringer,²⁹ A. Bhatti,⁵¹
M. Binkley,¹⁸ D. Bisello^u,⁴⁴ I. Bizjak,³¹ R.E. Blair,² C. Blocker,⁷ B. Blumenfeld,²⁶ A. Bocci,¹⁷ A. Bodek,⁵⁰
V. Boisvert,⁵⁰ G. Bolla,⁴⁹ D. Bortoletto,⁴⁹ J. Boudreau,⁴⁸ A. Boveia,¹¹ B. Brau,¹¹ A. Bridgeman,²⁵ L. Brigliadori,⁴⁴
C. Bromberg,³⁶ E. Brubaker,¹⁴ J. Budagov,¹⁶ H.S. Budd,⁵⁰ S. Budd,²⁵ K. Burkett,¹⁸ G. Busetto^u,⁴⁴ P. Bussey^x,²²
A. Buzatu,³⁴ K. L. Byrum,² S. Cabrera^p,¹⁷ C. Calancha,³² M. Campanelli,³⁶ M. Campbell,³⁵ F. Canelli,¹⁸
A. Canepa,⁴⁶ D. Carlsmith,⁶⁰ R. Carosi,⁴⁷ S. Carrillo^j,¹⁹ S. Carron,³⁴ B. Casal,¹² M. Casarsa,¹⁸ A. Castro^t,⁶
P. Catastini^r,⁴⁷ D. Cauz^w,⁵⁵ V. Cavaliere^r,⁴⁷ M. Cavalli-Sforza,⁴ A. Cerri,²⁹ L. Cerritoⁿ,³¹ S.H. Chang,²⁸
Y.C. Chen,¹ M. Chertok,⁸ G. Chiarelli,⁴⁷ G. Chlachidze,¹⁸ F. Chlebana,¹⁸ K. Cho,²⁸ D. Chokheli,¹⁶ J.P. Chou,²³
G. Choudalakis,³³ S.H. Chuang,⁵³ K. Chung,¹³ W.H. Chung,⁶⁰ Y.S. Chung,⁵⁰ C.I. Ciobanu,⁴⁵ M.A. Ciocci^r,⁴⁷
A. Clark,²¹ D. Clark,⁷ G. Compostella,⁴⁴ M.E. Convery,¹⁸ J. Conway,⁸ K. Copic,³⁵ M. Cordelli,²⁰ G. Cortiana^u,⁴⁴
D.J. Cox,⁸ F. Crescioli^q,⁴⁷ C. Cuenca Almenar^p,⁸ J. Cuevas^m,¹² R. Culbertson,¹⁸ J.C. Cully,³⁵ D. Dagenhart,¹⁸
M. Datta,¹⁸ T. Davies,²² P. de Barbaro,⁵⁰ S. De Cecco,⁵² A. Deisher,²⁹ G. De Lorenzo,⁴ M. Dell'Orso^q,⁴⁷
C. Deluca,⁴ L. Demortier,⁵¹ J. Deng,¹⁷ M. Deninno,⁶ P.F. Derwent,¹⁸ G.P. di Giovanni,⁴⁵ C. Dionisi^v,⁵²
B. Di Ruzza^w,⁵⁵ J.R. Dittmann,⁵ M. D'Onofrio,⁴ S. Donati^q,⁴⁷ P. Dong,⁹ J. Donini,⁴⁴ T. Dorigo,⁴⁴ S. Dube,⁵³
J. Efron,⁴⁰ A. Elagin,⁵⁴ R. Erbacher,⁸ D. Errede,²⁵ S. Errede,²⁵ R. Eusebi,¹⁸ H.C. Fang,²⁹ S. Farrington,⁴³
W.T. Fedorko,¹⁴ R.G. Feild,⁶¹ M. Feindt,²⁷ J.P. Fernandez,³² C. Ferrazza^s,⁴⁷ R. Field,¹⁹ G. Flanagan,⁴⁹ R. Forrest,⁸
M. Franklin,²³ J.C. Freeman,¹⁸ I. Furic,¹⁹ M. Gallinaro,⁵² J. Galyardt,¹³ F. Garbersen,¹¹ J.E. Garcia,⁴⁷
A.F. Garfinkel,⁴⁹ K. Genser,¹⁸ H. Gerberich,²⁵ D. Gerdes,³⁵ A. Gessler,²⁷ S. Giagu^v,⁵² V. Giakoumopoulou,³
P. Giannetti,⁴⁷ K. Gibson,⁴⁸ J.L. Gimmell,⁵⁰ C.M. Ginsburg,¹⁸ N. Giokaris,³ M. Giordani^w,⁵⁵ P. Giromini,²⁰
M. Giunta^q,⁴⁷ G. Giurgiu,²⁶ V. Glagolev,¹⁶ D. Glenzinski,¹⁸ M. Gold,³⁸ N. Goldschmidt,¹⁹ A. Golossanov,¹⁸
G. Gomez,¹² G. Gomez-Ceballos,³³ M. Goncharov,⁵⁴ O. González,³² I. Gorelov,³⁸ A.T. Goshaw,¹⁷ K. Goulianos,⁵¹
A. Gresele^u,⁴⁴ S. Grinstein,²³ C. Grosso-Pilcher,¹⁴ R.C. Group,¹⁸ U. Grundler,²⁵ J. Guimaraes da Costa,²³
Z. Gunay-Unalan,³⁶ C. Haber,²⁹ K. Hahn,³³ S.R. Hahn,¹⁸ E. Halkiadakis,⁵³ B.-Y. Han,⁵⁰ J.Y. Han,⁵⁰ R. Handler,⁶⁰
F. Happacher,²⁰ K. Hara,⁵⁶ D. Hare,⁵³ M. Hare,⁵⁷ S. Harper,⁴³ R.F. Harr,⁵⁹ R.M. Harris,¹⁸ M. Hartz,⁴⁸
K. Hatakeyama,⁵¹ J. Hauser,⁹ C. Hays,⁴³ M. Heck,²⁷ A. Heijboer,⁴⁶ B. Heinemann,²⁹ J. Heinrich,⁴⁶ C. Henderson,³³
M. Herndon,⁶⁰ J. Heuser,²⁷ S. Hewamanage,⁵ D. Hidas,¹⁷ C.S. Hill^c,¹¹ D. Hirschbuehl,²⁷ A. Hocker,¹⁸ S. Hou,¹
M. Houlden,³⁰ S.-C. Hsu,¹⁰ B.T. Huffman,⁴³ R.E. Hughes,⁴⁰ U. Husemann,⁶¹ J. Huston,³⁶ J. Incandela,¹¹
G. Introzzi,⁴⁷ M. Iori^v,⁵² A. Ivanov,⁸ E. James,¹⁸ B. Jayatilaka,¹⁷ E.J. Jeon,²⁸ M.K. Jha,⁶ S. Jindariani,¹⁸
W. Johnson,⁸ M. Jones,⁴⁹ K.K. Joo,²⁸ S.Y. Jun,¹³ J.E. Jung,²⁸ T.R. Junk,¹⁸ T. Kamon,⁵⁴ D. Kar,¹⁹ P.E. Karchin,⁵⁹
Y. Kato,⁴² R. Kephart,¹⁸ J. Keung,⁴⁶ V. Khotilovich,⁵⁴ B. Kilminster,⁴⁰ D.H. Kim,²⁸ H.S. Kim,²⁸ J.E. Kim,²⁸
M.J. Kim,²⁰ S.B. Kim,²⁸ S.H. Kim,⁵⁶ Y.K. Kim,¹⁴ N. Kimura,⁵⁶ L. Kirsch,⁷ S. Klimentenko,¹⁹ B. Knuteson,³³
B.R. Ko,¹⁷ S.A. Koay,¹¹ K. Kondo,⁵⁸ D.J. Kong,²⁸ J. Konigsberg,¹⁹ A. Korytov,¹⁹ A.V. Kotwal,¹⁷ M. Kreps,²⁷
J. Kroll,⁴⁶ D. Krop,¹⁴ N. Krumnack,⁵ M. Kruse,¹⁷ V. Krutelyov,¹¹ T. Kubo,⁵⁶ T. Kuhr,²⁷ N.P. Kulkarni,⁵⁹
M. Kurata,⁵⁶ Y. Kusakabe,⁵⁸ S. Kwang,¹⁴ A.T. Laasanen,⁴⁹ S. Lami,⁴⁷ S. Lammel,¹⁸ M. Lancaster,³¹ R.L. Lander,⁸
K. Lannon,⁴⁰ A. Lath,⁵³ G. Latino^r,⁴⁷ I. Lazzizzera^u,⁴⁴ T. LeCompte,² E. Lee,⁵⁴ S.W. Lee^o,⁵⁴ S. Leone,⁴⁷
J.D. Lewis,¹⁸ C.S. Lin,²⁹ J. Linacre,⁴³ M. Lindgren,¹⁸ E. Lipeles,¹⁰ A. Lister,⁸ D.O. Litvintsev,¹⁸ C. Liu,⁴⁸ T. Liu,¹⁸
N.S. Lockyer,⁴⁶ A. Loginov,⁶¹ M. Loretini^u,⁴⁴ L. Lovas,¹⁵ R.-S. Lu,¹ D. Lucchesi^u,⁴⁴ J. Lueck,²⁷ C. Luci^v,⁵²
P. Lujan,²⁹ P. Lukens,¹⁸ G. Lungu,⁵¹ L. Lyons,⁴³ J. Lys,²⁹ R. Lysak,¹⁵ E. Lytken,⁴⁹ P. Mack,²⁷ D. MacQueen,³⁴
R. Madrak,¹⁸ K. Maeshima,¹⁸ K. Makhoul,³³ T. Maki,²⁴ P. Maksimovic,²⁶ S. Malde,⁴³ S. Malik,³¹ G. Manca,³⁰
A. Manousakakis-Katsikakis,³ F. Margaroli,⁴⁹ C. Marino,²⁷ C.P. Marino,²⁵ A. Martin,⁶¹ V. Martinⁱ,²² M. Martínez,⁴
R. Martínez-Ballarín,³² T. Maruyama,⁵⁶ P. Mastrandrea,⁵² T. Masubuchi,⁵⁶ M.E. Mattson,⁵⁹ P. Mazzanti,⁶
K.S. McFarland,⁵⁰ P. McIntyre,⁵⁴ R. McNulty^h,³⁰ A. Mehta,³⁰ P. Mehtala,²⁴ A. Menzione,⁴⁷ P. Merkel,⁴⁹
C. Mesropian,⁵¹ T. Miao,¹⁸ N. Miladinovic,⁷ R. Miller,³⁶ C. Mills,²³ M. Milnik,²⁷ A. Mitra,¹ G. Mitselmakher,¹⁹
H. Miyake,⁵⁶ N. Moggi,⁶ C.S. Moon,²⁸ R. Moore,¹⁸ M.J. Morello^q,⁴⁷ J. Morlok,²⁷ P. Movilla Fernandez,¹⁸
J. Mülmenstädt,²⁹ A. Mukherjee,¹⁸ Th. Muller,²⁷ R. Mumford,²⁶ P. Murat,¹⁸ M. Mussini^t,⁶ J. Nachtman,¹⁸
Y. Nagai,⁵⁶ A. Nagano,⁵⁶ J. Naganoma,⁵⁸ K. Nakamura,⁵⁶ I. Nakano,⁴¹ A. Napier,⁵⁷ V. Necula,¹⁷ C. Neu,⁴⁶
M.S. Neubauer,²⁵ J. Nielsen^e,²⁹ L. Nodulman,² M. Norman,¹⁰ O. Norniella,²⁵ E. Nurse,³¹ L. Oakes,⁴³ S.H. Oh,¹⁷

Y.D. Oh,²⁸ I. Oksuzian,¹⁹ T. Okusawa,⁴² R. Orava,²⁴ K. Osterberg,²⁴ S. Pagan Griso^u,⁴⁴ C. Pagliarone,⁴⁷ E. Palencia,¹⁸ V. Papadimitriou,¹⁸ A. Papaikonomou,²⁷ A.A. Paramonov,¹⁴ B. Parks,⁴⁰ S. Pashapour,³⁴ J. Patrick,¹⁸ G. Pauletta^w,⁵⁵ M. Paulini,¹³ C. Paus,³³ D.E. Pellett,⁸ A. Penzo,⁵⁵ T.J. Phillips,¹⁷ G. Piacentino,⁴⁷ E. Pianori,⁴⁶ L. Pina,¹⁹ K. Pitts,²⁵ C. Plager,⁹ L. Pondrom,⁶⁰ O. Poukhov,¹⁶ N. Pounder,⁴³ F. Prakhoshyn,¹⁶ A. Pronko,¹⁸ J. Proudfoot,² F. Ptohos^g,¹⁸ E. Pueschel,¹³ G. Punzi^q,⁴⁷ J. Pursley,⁶⁰ J. Rademacker^c,⁴³ A. Rahaman,⁴⁸ V. Ramakrishnan,⁶⁰ N. Ranjan,⁴⁹ I. Redondo,³² B. Reisert,¹⁸ V. Rekovic,³⁸ P. Renton,⁴³ M. Rescigno,⁵² S. Richter,²⁷ F. Rimondi^t,⁶ L. Ristori,⁴⁷ A. Robson,²² T. Rodrigo,¹² T. Rodriguez,⁴⁶ E. Rogers,²⁵ S. Rolli,⁵⁷ R. Roser,¹⁸ M. Rossi,⁵⁵ R. Rossin,¹¹ P. Roy,³⁴ A. Ruiz,¹² J. Russ,¹³ V. Rusu,¹⁸ H. Saarikko,²⁴ A. Safonov,⁵⁴ W.K. Sakumoto,⁵⁰ O. Saltó,⁴ D. Saltzberg,⁹ L. Santi^w,⁵⁵ S. Sarkar^v,⁵² L. Sartori,⁴⁷ K. Sato,¹⁸ A. Savoy-Navarro,⁴⁵ T. Scheidle,²⁷ P. Schlabach,¹⁸ A. Schmidt,²⁷ E.E. Schmidt,¹⁸ M.A. Schmidt,¹⁴ M.P. Schmidt^{*},⁶¹ M. Schmitt,³⁹ T. Schwarz,⁸ L. Scodellaro,¹² A.L. Scott,¹¹ A. Scribano^r,⁴⁷ F. Scuri,⁴⁷ A. Sedov,⁴⁹ S. Seidel,³⁸ Y. Seiya,⁴² A. Semenov,¹⁶ L. Sexton-Kennedy,¹⁸ A. Sfyrla,²¹ S.Z. Shalhout,⁵⁹ T. Shears,³⁰ P.F. Shepard,⁴⁸ D. Sherman,²³ M. Shimojima^l,⁵⁶ S. Shiraishi,¹⁴ M. Shochet,¹⁴ Y. Shon,⁶⁰ I. Shreyber,³⁷ A. Sidoti,⁴⁷ P. Sinervo,³⁴ A. Sisakyan,¹⁶ A.J. Slaughter,¹⁸ J. Slaunwhite,⁴⁰ K. Sliwa,⁵⁷ J.R. Smith,⁸ F.D. Snider,¹⁸ R. Snihur,³⁴ A. Soha,⁸ S. Somalwar,⁵³ V. Sorin,³⁶ J. Spalding,¹⁸ T. Spreitzer,³⁴ P. Squillacioti^r,⁴⁷ M. Stanitzki,⁶¹ R. St. Denis,²² B. Stelzer,⁹ O. Stelzer-Chilton,⁴³ D. Stentz,³⁹ J. Strologas,³⁸ D. Stuart,¹¹ J.S. Suh,²⁸ A. Sukhanov,¹⁹ M. Sutherland,⁹ I. Suslov,¹⁶ T. Suzuki,⁵⁶ A. Taffard^d,²⁵ R. Takashima,⁴¹ Y. Takeuchi,⁵⁶ R. Tanaka,⁴¹ M. Tecchio,³⁵ P.K. Teng,¹ K. Terashi,⁵¹ J. Thom^f,¹⁸ A.S. Thompson,²² G.A. Thompson,²⁵ E. Thomson,⁴⁶ P. Tipton,⁶¹ V. Tiwari,¹³ S. Tkaczyk,¹⁸ D. Toback,⁵⁴ S. Tokar,¹⁵ K. Tollefson,³⁶ T. Tomura,⁵⁶ D. Tonelli,¹⁸ S. Torre,²⁰ D. Torretta,¹⁸ P. Totaro^w,⁵⁵ S. Tourneur,⁴⁵ Y. Tu,⁴⁶ N. Turini^r,⁴⁷ F. Ukegawa,⁵⁶ S. Vallecorsa,²¹ N. van Remortel^a,²⁴ A. Varganov,³⁵ E. Vataga^s,⁴⁷ F. Vázquez^j,¹⁹ G. Velev,¹⁸ C. Vellidis,³ V. Veszpremi,⁴⁹ M. Vidal,³² R. Vidal,¹⁸ I. Vila,¹² R. Vilar,¹² T. Vine,³¹ M. Vogel,³⁸ I. Volobouev^o,²⁹ G. Volpi^q,⁴⁷ F. Würthwein,¹⁰ P. Wagner,² R.G. Wagner,² R.L. Wagner,¹⁸ J. Wagner-Kuhr,²⁷ W. Wagner,²⁷ T. Wakisaka,⁴² R. Wallny,⁹ S.M. Wang,¹ A. Warburton,³⁴ D. Waters,³¹ M. Weinberger,⁵⁴ W.C. Wester III,¹⁸ B. Whitehouse,⁵⁷ D. Whiteson^d,⁴⁶ A.B. Wicklund,² E. Wicklund,¹⁸ G. Williams,³⁴ H.H. Williams,⁴⁶ P. Wilson,¹⁸ B.L. Winer,⁴⁰ P. Wittich^f,¹⁸ S. Wolbers,¹⁸ C. Wolfe,¹⁴ T. Wright,³⁵ X. Wu,²¹ S.M. Wynne,³⁰ A. Yagil,¹⁰ K. Yamamoto,⁴² J. Yamaoka,⁵³ U.K. Yang^k,¹⁴ Y.C. Yang,²⁸ W.M. Yao,²⁹ G.P. Yeh,¹⁸ J. Yoh,¹⁸ K. Yorita,¹⁴ T. Yoshida,⁴² G.B. Yu,⁵⁰ I. Yu,²⁸ S.S. Yu,¹⁸ J.C. Yun,¹⁸ L. Zanello^v,⁵² A. Zanetti,⁵⁵ I. Zaw,²³ X. Zhang,²⁵ Y. Zheng^b,⁹ and S. Zucchelli^{t6}

(CDF Collaboration[†])

The CDF Collaboration

¹*Institute of Physics, Academia Sinica, Taipei, Taiwan 11529, Republic of China*

²*Argonne National Laboratory, Argonne, Illinois 60439*

³*University of Athens, 157 71 Athens, Greece*

⁴*Institut de Fisica d'Altes Energies, Universitat Autònoma de Barcelona, E-08193, Bellaterra (Barcelona), Spain*

⁵*Baylor University, Waco, Texas 76798*

⁶*Istituto Nazionale di Fisica Nucleare Bologna, ⁴University of Bologna, I-40127 Bologna, Italy*

⁷*Brandeis University, Waltham, Massachusetts 02254*

⁸*University of California, Davis, Davis, California 95616*

⁹*University of California, Los Angeles, Los Angeles, California 90024*

¹⁰*University of California, San Diego, La Jolla, California 92093*

¹¹*University of California, Santa Barbara, Santa Barbara, California 93106*

¹²*Instituto de Fisica de Cantabria, CSIC-University of Cantabria, 39005 Santander, Spain*

¹³*Carnegie Mellon University, Pittsburgh, PA 15213*

¹⁴*Enrico Fermi Institute, University of Chicago, Chicago, Illinois 60637*

¹⁵*Comenius University, 842 48 Bratislava, Slovakia; Institute of Experimental Physics, 040 01 Kosice, Slovakia*

¹⁶*Joint Institute for Nuclear Research, RU-141980 Dubna, Russia*

¹⁷*Duke University, Durham, North Carolina 27708*

¹⁸*Fermi National Accelerator Laboratory, Batavia, Illinois 60510*

¹⁹*University of Florida, Gainesville, Florida 32611*

²⁰*Laboratori Nazionali di Frascati, Istituto Nazionale di Fisica Nucleare, I-00044 Frascati, Italy*

²¹*University of Geneva, CH-1211 Geneva 4, Switzerland*

²²*Glasgow University, Glasgow G12 8QQ, United Kingdom*

²³*Harvard University, Cambridge, Massachusetts 02138*

²⁴*Division of High Energy Physics, Department of Physics,*

University of Helsinki and Helsinki Institute of Physics, FIN-00014, Helsinki, Finland

²⁵*University of Illinois, Urbana, Illinois 61801*

²⁶*The Johns Hopkins University, Baltimore, Maryland 21218*

²⁷*Institut für Experimentelle Kernphysik, Universität Karlsruhe, 76128 Karlsruhe, Germany*

- ²⁸Center for High Energy Physics: Kyungpook National University, Daegu 702-701, Korea; Seoul National University, Seoul 151-742, Korea; Sungkyunkwan University, Suwon 440-746, Korea; Korea Institute of Science and Technology Information, Daejeon, 305-806, Korea; Chonnam National University, Gwangju, 500-757, Korea
- ²⁹Ernest Orlando Lawrence Berkeley National Laboratory, Berkeley, California 94720
- ³⁰University of Liverpool, Liverpool L69 7ZE, United Kingdom
- ³¹University College London, London WC1E 6BT, United Kingdom
- ³²Centro de Investigaciones Energeticas Medioambientales y Tecnologicas, E-28040 Madrid, Spain
- ³³Massachusetts Institute of Technology, Cambridge, Massachusetts 02139
- ³⁴Institute of Particle Physics: McGill University, Montréal, Canada H3A 2T8; and University of Toronto, Toronto, Canada M5S 1A7
- ³⁵University of Michigan, Ann Arbor, Michigan 48109
- ³⁶Michigan State University, East Lansing, Michigan 48824
- ³⁷Institution for Theoretical and Experimental Physics, ITEP, Moscow 117259, Russia
- ³⁸University of New Mexico, Albuquerque, New Mexico 87131
- ³⁹Northwestern University, Evanston, Illinois 60208
- ⁴⁰The Ohio State University, Columbus, Ohio 43210
- ⁴¹Okayama University, Okayama 700-8530, Japan
- ⁴²Osaka City University, Osaka 588, Japan
- ⁴³University of Oxford, Oxford OX1 3RH, United Kingdom
- ⁴⁴Istituto Nazionale di Fisica Nucleare, Sezione di Padova-Trento, ^uUniversity of Padova, I-35131 Padova, Italy
- ⁴⁵LPNHE, Université Pierre et Marie Curie/IN2P3-CNRS, UMR7585, Paris, F-75252 France
- ⁴⁶University of Pennsylvania, Philadelphia, Pennsylvania 19104
- ⁴⁷Istituto Nazionale di Fisica Nucleare Pisa, ^qUniversity of Pisa, ^rUniversity of Siena and ^sScuola Normale Superiore, I-56127 Pisa, Italy
- ⁴⁸University of Pittsburgh, Pittsburgh, Pennsylvania 15260
- ⁴⁹Purdue University, West Lafayette, Indiana 47907
- ⁵⁰University of Rochester, Rochester, New York 14627
- ⁵¹The Rockefeller University, New York, New York 10021
- ⁵²Istituto Nazionale di Fisica Nucleare, Sezione di Roma 1, ^vSapienza Università di Roma, I-00185 Roma, Italy
- ⁵³Rutgers University, Piscataway, New Jersey 08855
- ⁵⁴Texas A&M University, College Station, Texas 77843
- ⁵⁵Istituto Nazionale di Fisica Nucleare Trieste/ Udine, ^wUniversity of Trieste/ Udine, Italy
- ⁵⁶University of Tsukuba, Tsukuba, Ibaraki 305, Japan
- ⁵⁷Tufts University, Medford, Massachusetts 02155
- ⁵⁸Waseda University, Tokyo 169, Japan
- ⁵⁹Wayne State University, Detroit, Michigan 48201
- ⁶⁰University of Wisconsin, Madison, Wisconsin 53706
- ⁶¹Yale University, New Haven, Connecticut 06520
- (Dated: October 30, 2018)

We report a search for the flavor changing neutral current (FCNC) decay of the top quark $t \rightarrow Zq$ ($q = u, c$) in $p\bar{p}$ collisions at $\sqrt{s} = 1.96$ TeV using a data sample corresponding to an integrated luminosity of 1.9 fb^{-1} collected by the CDF II detector. This decay is strongly suppressed in the standard model (SM) and an observation of a signal at the Tevatron would be an indication of physics beyond the SM. Using $Z+ \geq 4$ jet final state candidate events, both with and without an identified bottom quark jet, we discriminate signal from background by exploiting kinematic constraints present in FCNC events and obtain an upper limit of $\mathcal{B}(t \rightarrow Zq) < 3.7\%$ at 95% C.L.

PACS numbers: 13.85.Qk 12.60.Jv 13.85.Rm 14.80.Ly 13.85-t

*Deceased

†With visitors from ^aUniversiteit Antwerpen, B-2610 Antwerp, Belgium, ^bChinese Academy of Sciences, Beijing 100864, China, ^cUniversity of Bristol, Bristol BS8 1TL, United Kingdom, ^dUniversity of California Irvine, Irvine, CA 92697, ^eUniversity of California Santa Cruz, Santa Cruz, CA 95064, ^fCornell University, Ithaca, NY 14853, ^gUniversity of Cyprus, Nicosia CY-1678, Cyprus, ^hUniversity College Dublin, Dublin 4, Ireland, ⁱUniversity of Edinburgh, Edinburgh EH9 3JZ, United Kingdom, ^jUniversidad

Iberoamericana, Mexico D.F., Mexico, ^kUniversity of Manchester, Manchester M13 9PL, England, ^lNagasaki Institute of Applied Science, Nagasaki, Japan, ^mUniversity de Oviedo, E-33007 Oviedo, Spain, ⁿQueen Mary, University of London, London, E1 4NS, England, ^oTexas Tech University, Lubbock, TX 79409, ^pIFIC(CSIC-Universitat de Valencia), 46071 Valencia, Spain, ^qRoyal Society of Edinburgh/Scottish Executive Support Research Fellow,

Flavor changing neutral current (FCNC) interactions, which mediate transitions from one type of quark to another with the same electric charge, are suppressed in the standard model of particle physics (SM). FCNC processes are therefore sensitive indicators of physics beyond the SM (BSM). Presently there are only loose experimental bounds on FCNC decays of the t (top) quark [1], the heaviest known quark. While the SM branching fraction for $t \rightarrow Zq$ ($q = u, c$) is predicted to be $\mathcal{O}(10^{-14})$ [2], BSM models such as supersymmetry and quark compositeness allow branching fractions as high as $\mathcal{O}(10^{-4})$ [2, 3]. An observation of the top FCNC decay $t \rightarrow Zq$ with present-size data samples would be a strong indication of BSM physics.

In Tevatron Run I, a CDF search for the $t \rightarrow Zq$ decay yielded the branching fraction upper limit $\mathcal{B}(t \rightarrow Zq) < 33\%$ (95% C.L.) [4]. The current best 95% C.L. upper limit on $\mathcal{B}(t \rightarrow Zq)$, 13.7%, was set by the L3 experiment [5] from the non-observation of FCNC single t quark production. These analyses assumed a t quark mass of $m_t = 175 \text{ GeV}/c^2$, close to the current world average of $m_t = 172.4 \pm 1.2 \text{ GeV}/c^2$ [6]. In this Letter we also assume $m_t = 175 \text{ GeV}/c^2$ and evaluate the small effect of different m_t on the result.

We present the first Tevatron Run II search for the top FCNC decay $t \rightarrow Zq$ in $t\bar{t}$ pairs. The data sample analyzed for this Letter corresponds to an integrated luminosity of 1.9 fb^{-1} of $p\bar{p}$ collisions at $\sqrt{s} = 1.96 \text{ TeV}$, collected by the CDF II detector from March 2002 to May 2007. Our primary signal signature consists of the FCNC decay $t \rightarrow Zq$ ($q = u, c$) together with the dominant SM decay $\bar{t} \rightarrow W^- \bar{b}$ (charge conjugate modes are implied). We search for the Z boson via its decays $Z \rightarrow e^+e^-$ and $Z \rightarrow \mu^+\mu^-$ and for the decay of the W boson into a quark-antiquark pair. Two leptons and at least four jets of hadrons, coming from the four quarks from secondary decays, can be observed in the detector. We also allow for events in which both t quarks undergo FCNC decays. We consider several SM background processes that also result in final states with a reconstructed Z boson and four or more jets. The dominant background process is the production of Z bosons with associated jets (Z +jets). Smaller contributions come from SM $t\bar{t}$ production and the production of pairs of gauge bosons (dibosons), WZ and ZZ . The contributions from WW diboson production and from W bosons produced in association with jets are negligible.

The components of the CDF II detector relevant to this analysis are briefly described here; a more complete description can be found elsewhere [7]. The transverse momenta p_T and pseudorapidities η [8] of charged particles are measured by a silicon strip detector [9] and a 96-layer drift chamber (COT) [10] inside a 1.4 T solenoidal magnetic field. The silicon detector and the COT provide good combined reconstruction efficiency for $|\eta| < 1.2$. The precise position resolution of the silicon detector is also crucial for identifying displaced secondary vertices from long-lived B hadrons (b -tagging). Electromagnetic (EM) and hadronic calorimeters measure energies

of charged and neutral particles in the central ($|\eta| < 1.1$) and end-plug ($1.1 < |\eta| < 3.6$) regions. Drift chambers and scintillation counters located on the rear of the calorimeters and behind an additional steel absorber detect muons with $|\eta| < 1.0$. A three level trigger selects events that contain electrons (muons) with $E_T > 18 \text{ GeV}$ ($p_T > 18 \text{ GeV}/c$).

We use the PYTHIA v6.216 Monte Carlo (MC) generator [11] to simulate the FCNC signal in $t\bar{t}$ events and all sources of SM background, except Z +jets production, whose kinematic distributions we simulate with the ALPGEN MC generator [12], v2.10' interfaced to PYTHIA v6.325. Acceptance, efficiency, and kinematic distributions of signal and background are determined from the above MC simulations. We add a $t \rightarrow Zq$ decay channel to PYTHIA by forcing the Z helicity to be consistent with the expectation from an SM-like Higgs mechanism of 65% longitudinally polarized and 35% left-handed Z bosons. The main signal MC sample contains events that decay according to our primary signature, $t\bar{t} \rightarrow ZqWb$ with $q = c$. If the $t \rightarrow Zc$ decay is replaced by $t \rightarrow Zu$, the probability to b -tag an FCNC signal event is reduced from 50% to 45%, where we apply the SecVtx algorithm [7] for the b -tagging. We have also generated an MC event sample in which both t quarks decay via the FCNC mode and the Z is allowed to decay into the e^+e^- , $\mu^+\mu^-$, and $q\bar{q}$ decay modes. The amount of $t\bar{t} \rightarrow ZcZc$ relative to $t\bar{t} \rightarrow WbZc$ is adjusted according to the branching fraction $\mathcal{B}(t \rightarrow Zq)$ during the limit calculation.

We apply corrections for trigger efficiencies and for different efficiencies in data and simulation for lepton identification and reconstruction, b -tagging, and misidentification of secondary vertices (mistags).

The analysis proceeds in three steps. Our base selection requires a Z boson and four or more jets. An optimized event selection separates the FCNC signal from the SM backgrounds based on kinematic properties of the event. All events that pass the optimized selection are further divided into two signal regions based on whether any of the four leading jets has an identified b -jet (“ b -tagged region”) or not (“non- b -tagged region”); those events that pass the base selection but not the optimized selection are placed in a “control” region. While only 12% of FCNC signal acceptance falls in the control region, two-thirds of the SM backgrounds are located there. We finally fit the data to one-dimensional probability density histograms (“templates”) of one of the kinematic distributions (mass χ^2 , see below) to derive a limit on $\mathcal{B}(t \rightarrow Zq)$. This is illustrated in Fig. 1. To reduce systematic uncertainties, the measurement is normalized to the measured event yield in SM $t\bar{t}$ production.

Our base selection chooses events with two oppositely-charged leptons of the same flavor (e or μ) and four or more jets. One lepton is required to be a central electron or muon, the other can be a forward electron or a track, as described below. The leptons must be compatible with originating from a Z boson in the mass window from $76 \text{ GeV}/c^2$ to $106 \text{ GeV}/c^2$ ($> 3\sigma$ in units of CDF’s Z

mass resolution).

All leptons used in this analysis are required to be well isolated in a cone of $\Delta R = \sqrt{(\Delta\eta)^2 + (\Delta\phi)^2} < 0.4$ [8] and to have transverse energies E_T (momenta p_T) greater than 20 GeV (20 GeV/ c). Electrons are identified by requiring an energy cluster in the EM calorimeter with a single track pointing to it. Central electrons are required to have a high quality COT-based track, calorimeter cluster E_T consistent with the track p_T , a high fraction of the total energy deposition in the EM calorimeter, and a lateral shower profile consistent with electron showers. Forward electrons are reconstructed in the end-plug calorimeter and have similar constraints except that the tracks are reconstructed only in the silicon detector and the calorimeter cluster E_T and track p_T are not compared. Muons are identified by matching tracks reconstructed in the COT to track segments reconstructed in the muon chambers and by requiring energy depositions in the calorimeters consistent with minimum ionizing particles. The muons in this analysis are required to be in the central region ($|\eta| < 1.0$). We double the acceptance for leptonic Z decays by allowing one of the two lepton candidates to satisfy weaker selection criteria, requiring only an isolated track which passes COT and silicon detector track quality cuts. For tracks used as electrons, if an EM calorimeter tower is associated to the track and the energy of the EM tower is greater than the track momentum, the EM tower energy is used instead of the track momentum.

Jets are identified by energy deposited in the calorimeters within a cone of $\Delta R < 0.4$. To improve the parton energy estimate, jets are corrected for instrumental effects [13]. We select events with at least four jets with corrected $E_T > 15$ GeV and $|\eta| < 2.4$.

We separate the FCNC signal from the MC background with the help of further selection criteria in addition to the above base selection that will form the optimized selection, a mass χ^2 , the transverse mass of the system, and the E_T of the four leading (highest E_T) jets.

The decay $t\bar{t} \rightarrow WbZq \rightarrow q\bar{q}'b\ell\ell q''$ contains no high-energy neutrinos; therefore we can fully reconstruct the event kinematics. The four jets in signal events result from the b quark and the decay products of the W in the $t \rightarrow Wb$ decay, and the c or u quark from the $t \rightarrow Zq$ decay. We form all permutations of the four leading jets in the events to compare the reconstructed masses (m_{rec}) of the W , top quark decaying to Wb , and top quark decaying to Zq . We define a mass χ^2 as

$$\chi^2 = \left(\frac{m_{W,\text{rec}} - m_W}{\sigma_W} \right)^2 + \left(\frac{m_{t \rightarrow Wb,\text{rec}} - m_t}{\sigma_{t \rightarrow Wb}} \right)^2 + \left(\frac{m_{t \rightarrow Zq,\text{rec}} - m_t}{\sigma_{t \rightarrow Zq}} \right)^2, \quad (1)$$

and select the permutation with the smallest χ^2 . We scale the measured four-momenta of the W and Z boson daughter particles such that the boson masses are fixed to the world average values [14] and use the scaled four-

momenta to calculate the two top quark masses. The widths used are given by the standard deviations of the reconstructed masses measured in the MC simulation of FCNC events. Using the correct pairing of jets to partons, we extract $\sigma_W = 15$ GeV/ c^2 , $\sigma_{t \rightarrow Wb} = 24$ GeV/ c^2 , and $\sigma_{t \rightarrow Zq} = 21$ GeV/ c^2 . We expect FCNC signal events to populate the low χ^2 region and background events to result in higher χ^2 , see Fig. 1. We have verified that the components of Eq. (1) describe the data well in events with a Z boson and three jets.

Since the FCNC signal events originate from $t\bar{t}$ decays, they contain more central Z bosons and jets than background events. To exploit this, we use the transverse mass of the Z and the four leading jets, defined as $m_T = \sqrt{(\sum E_T)^2 - (\sum \vec{p}_T)^2}$, as a selection criterion. We also apply a tiered cut on the E_T of the four leading jets, as FCNC signal events contain jets with higher transverse momenta than SM background events.

We optimized these additional selection criteria for the best expected limit on $\mathcal{B}(t \rightarrow Zq)$ in the absence of a signal, using the MC simulation and a signal-depleted control region in the data ($\sqrt{\chi^2} > 3$). The optimization was performed in the blind phase of a counting experiment analysis using the first 1.1 fb $^{-1}$ of integrated luminosity [15]. We leave the optimized selection unchanged for the full 1.9 fb $^{-1}$ result; it requires transverse mass $m_T \geq 200$ GeV/ c^2 , leading jet $E_T \geq 40$ GeV, second jet $E_T \geq 30$ GeV, third jet $E_T \geq 20$ GeV, and fourth jet $E_T \geq 15$ GeV. After optimization, 88% of the FCNC signal events from the base selection fall into the two signal regions, compared to 33% of the background events. The inclusive signal acceptances for the decay $t\bar{t} \rightarrow WbZc$ ($t\bar{t} \rightarrow ZcZc$) are 0.43% (0.58%) for the b -tagged selection, 0.34% (0.86%) for the non- b -tagged selection, and 0.10% (0.16%) for the control region.

To determine the FCNC branching fraction, we take into account single or double FCNC decays of $t\bar{t}$ pairs and normalize to the event yield of a selection for the SM decay $t\bar{t} \rightarrow WbWb \rightarrow \ell\nu b q\bar{q}'b$ (“lepton+jets”) requiring at least two jets to be secondary vertex b -tagged [16]. In 1.9 fb $^{-1}$ we observe 277 $t\bar{t}$ candidate events, consistent with a production cross section of 8.8 ± 0.7 (stat.) pb assuming $\mathcal{B}(t \rightarrow Wb) = 100\%$. If $t \rightarrow Zq$ decays were present, these additional $t\bar{t}$ decays are less likely to be reconstructed in the lepton+jets mode, resulting in a measured $t\bar{t}$ production cross section smaller than the actual cross section. We correct for this effect by modifying the measured cross section based on the limit we set on $\mathcal{B}(t \rightarrow Zq)$.

We extract a limit on the branching fraction $\mathcal{B}(t \rightarrow Zq)$ from a fit to the mass χ^2 distribution using templates constructed from the MC simulated mass χ^2 distributions of the FCNC signal and the SM backgrounds (Z +jets, SM $t\bar{t}$, and dibosons). The normalization of the dominant Z +jets background is the most difficult to estimate from data and MC simulations; therefore it is extracted from the fit. The SM $t\bar{t}$ background is normalized to the observed event yield in the lepton+jets decay mode; back-

TABLE I: Results of the fit to data. From the ratio of the number of Z +jets events in the signal and the control regions and the tagging fraction f_{tag} , we obtain $Z_{\text{tagged}} = 13.5$ events and $Z_{\text{non-tagged}} = 53.9$ events.

Fit Parameter	Value
Branching Fraction, $\mathcal{B}(t \rightarrow Zq)$ (%)	-1.49 ± 1.52
Z +Jets Events in Control Region, Z_{control}	129.0 ± 11.1
Ratio Signal/Control Region, \mathcal{R}_{sig}	0.52 ± 0.07
Tagging Fraction, f_{tag}	0.20 ± 0.06
Jet Energy Scale Shift, σ_{JES}	-0.74 ± 0.43

grounds from diboson production are normalized to their theoretical cross sections. Both contributions are fixed in the fit. The expected background from SM $t\bar{t}$ production and diboson production is 2.2 ± 0.2 (3.2 ± 0.2) events for the b -tagged (non- b -tagged) selection. The b -tagged, the non- b -tagged, and the control region are fit simultaneously. We include systematic uncertainties due to the shapes of the signal and background templates by allowing the templates to change shape via a histogram interpolation technique (horizontal template morphing) [17]. The uncertainty due to the experimental jet energy scale (JES) is more than three times larger than any other uncertainty, and the data are most consistent with a shift of the JES; therefore we only include JES induced shape uncertainties in the fitting procedure.

We use the signal-depleted control region to constrain the background shape uncertainties without losing sensitivity to a small FCNC signal. Additionally we use the number of Z +jets events observed in the control region, Z_{control} , to place a loose constraint on the number of Z +jets events in the two signal regions, Z_{signal} . We constrain the ratio $\mathcal{R}_{\text{sig}} = Z_{\text{signal}}/Z_{\text{control}}$ to the value estimated by the MC simulation, $\mathcal{R}_{\text{sig}} = 0.51 \pm 0.10$ at the nominal JES. The uncertainty is conservatively estimated by varying the energy scales in the ALPGEN MC generator. We adjust \mathcal{R}_{sig} as a function of the JES shift σ_{JES} , keeping the relative uncertainty of 20%. The absolute number of Z +jets background events remains unconstrained. To reflect the constraint on \mathcal{R}_{sig} in the template fit, we parameterize the number of Z +jets events passing the b -tagged and non- b -tagged signal selections, Z_{tagged} and $Z_{\text{non-tagged}}$, as $Z_{\text{tagged}} = f_{\text{tag}} \cdot \mathcal{R}_{\text{sig}} \cdot Z_{\text{control}}$ and $Z_{\text{non-tagged}} = (1 - f_{\text{tag}}) \cdot \mathcal{R}_{\text{sig}} \cdot Z_{\text{control}}$, where f_{tag} is the fraction of Z +jets events passing the b -tagged signal selection. In summary, the unconstrained parameters of the template fit include the branching fraction $\mathcal{B}(t \rightarrow Zq)$, Z_{control} , the tagging fraction f_{tag} , and the shift in JES σ_{JES} . We apply a Gaussian constraint on the ratio \mathcal{R}_{sig} . From the template fit to the data we measure a branching fraction $\mathcal{B}(t \rightarrow Zq) = -1.49\%$. The fit result is summarized in Table I and in Fig. 1.

We employ a Feldman-Cousins (FC) limit calculation framework that includes the handling of systematic uncertainties [18]. The FC construction is based on applying the above template fits to simulated experiments that are generated taking into account all known sources of systematic rate and shape uncertainty and their correlations (systematic uncertainties are discussed in the

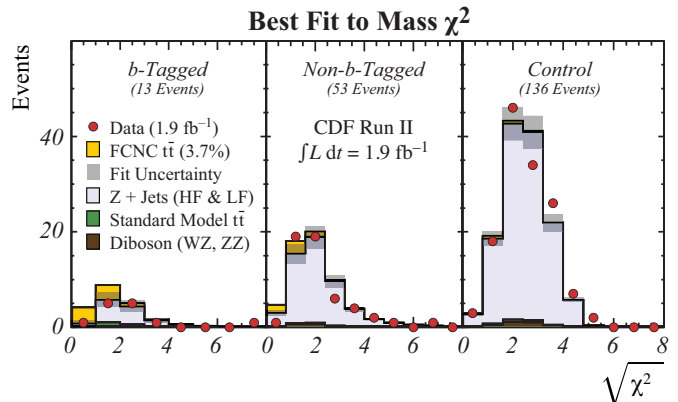


FIG. 1: Mass χ^2 distribution for b -tagged and non- b -tagged signal regions and the control region. The data points as a function of $\sqrt{\chi^2}$ are compared to the SM background prediction and the expected FCNC yield at the observed 95% C.L. upper limit on the branching fraction $\mathcal{B}(t \rightarrow Zq) < 3.7\%$. The data are consistent with the background prediction.

next paragraphs). We expect a limit of $(5.0 \pm 2.2)\%$ in the absence of signal. From the FC construction we find $\mathcal{B}(t \rightarrow Zq) < 3.7\%$ at 95% C.L.

We have studied systematic uncertainties due to shape uncertainties of the fitted templates, rate uncertainties (signal acceptance, background rate), and due to the normalization to the lepton+jets event yield. We treat the dominant source of template shape uncertainties, the experimental JES, as a free fit parameter. To account for further shape uncertainties, we measure the bias on the fitted branching fraction $\mathcal{B}(t \rightarrow Zq)$ in simulated experiments generated assuming the second largest source of shape uncertainties, the MC generator used for the Z +jets background. We simulate Z +jets events for which the vertex energy scale is varied by factors of two and assign the measured relative branching fraction bias at $\mathcal{B}(t \rightarrow Zq) = 3.7\%$ as a systematic uncertainty (5.6%).

The rate uncertainties, summarized in Table II are divided into anti-correlated uncertainties, those which cause migration of events between b -tagged and non- b -tagged selections, and correlated uncertainties, those which simultaneously increase or decrease both selections. The signal acceptance systematic uncertainties are evaluated for the ratio of the FCNC signal acceptance to the acceptance for the event selection used in the lepton+jets normalization mode. Background rate uncertainties affect only the smaller SM $t\bar{t}$ and diboson backgrounds. The rate of the dominant Z +jets background in the control region is a free parameter in the template fit; therefore we do not assign systematic uncertainties for this.

Normalization to the lepton+jets event yields in the $t\bar{t}$ production cross section analysis removes nearly all uncertainties depending directly on luminosity. Many other systematic uncertainties also partially cancel. We absorb the statistical and systematic uncertainties of the $t\bar{t}$ production cross section measurement as part of the systematic uncertainty (7.8%).

In conclusion, we have searched for the top quark flavor changing neutral current decay $t \rightarrow Zq$ in events with

TABLE II: Systematic uncertainties of the FCNC signal acceptance relative to the acceptance of the lepton+jets normalization mode and the background rate for the b -tagged and non- b -tagged selections.

Systematic Uncertainty	Acceptance		Background	
	b	Non- b	b	Non- b
ID, Trig, and PDF	1.0	1.0	1.5	1.5
Initial/Final State Rad.	4.8	5.5	—	—
Z Helicity	3.4	3.6	—	—
Total Correlated	6.2	6.1	6.2	6.2
b -Tagging	5.6	16.1	3.2	2.5
$\mathcal{B}(t \rightarrow Zc)$ vs. $\mathcal{B}(t \rightarrow Zu)$	4.5	4.5	—	—
Total Anti-Correlated	7.2	16.7	3.2	2.5

a Z boson and four or more jets using CDF Run II data corresponding to 1.9 fb^{-1} of integrated luminosity. The data are consistent with the SM background prediction, and we set an upper limit on the branching fraction $\mathcal{B}(t \rightarrow Zq)$ of 3.7% at 95% C.L. at a top quark mass of $175 \text{ GeV}/c^2$. Assuming a top quark mass of $170 \text{ GeV}/c^2$, the 95% C.L. upper limit is 4.1%. Compared with the previous world's best limit of 13.7% by the L3 experi-

ment [5] at LEP2, and the previous Tevatron upper limit of 33%, as reported by CDF Run I [4], our reported limit of 3.7% represents a substantial improvement.

We thank the Fermilab staff and the technical staffs of the participating institutions for their vital contributions. This work was supported by the U.S. Department of Energy and National Science Foundation; the Italian Istituto Nazionale di Fisica Nucleare; the Ministry of Education, Culture, Sports, Science and Technology of Japan; the Natural Sciences and Engineering Research Council of Canada; the National Science Council of the Republic of China; the Swiss National Science Foundation; the A.P. Sloan Foundation; the Bundesministerium für Bildung und Forschung, Germany; the Korean Science and Engineering Foundation and the Korean Research Foundation; the Science and Technology Facilities Council and the Royal Society, UK; the Institut National de Physique Nucleaire et Physique des Particules/CNRS; the Russian Foundation for Basic Research; the Comisión Interministerial de Ciencia y Tecnología, Spain; the European Community's Human Potential Programme; the Slovak R&D Agency; and the Academy of Finland.

-
- [1] H. Fritzsch, Phys. Lett. B **224**, 423 (1989).
[2] J. A. Aguilar-Saavedra, Acta Phys. Polon. B **35**, 2695 (2004).
[3] F. Larios, R. Martínez, M.A. Pérez, Int. J. Mod. Phys. A **21**, 3473 (2006).
[4] F. Abe *et al.* (CDF Collaboration), Phys. Rev. Lett. **80**, 2525 (1998).
[5] P. Achard *et al.* (L3 Collaboration), Phys. Lett. B **549**, 290 (2002).
[6] Tevatron Electroweak Working Group, arXiv:0808.1089 [hep-ex].
[7] D. Acosta *et al.* (CDF Collaboration), Phys. Rev. D **71**, 052003 (2005).
[8] In the CDF geometry, θ is the polar angle with respect to the proton beam axis (positive z direction), and ϕ is the azimuthal angle. The pseudorapidity is $\eta = -\ln[\tan(\theta/2)]$.
[9] A. Sill *et al.*, Nucl. Instrum. Methods A **447**, 1 (2000).
T. Affolder *et al.*, Nucl. Instrum. Methods A **453**, 84 (2000). C.S. Hill *et al.*, Nucl. Instrum. Methods A **511**, 118 (2003).
[10] T. Affolder *et al.*, Nucl. Instrum. Methods A **526**, 249 (2004).
[11] T. Sjöstrand *et al.*, Comput. Phys. Commun. **135**, 238 (2001).
[12] M. L. Mangano *et al.*, JHEP **07**, 001 (2003).
[13] A. Bhatti *et al.*, Nucl. Instrum. Methods A **566**, 2 (2006).
[14] W.-M. Yao *et al.*, J. Phys. G **33**, 1 (2006).
[15] For the 1.1 fb^{-1} blind analysis, we obtain a 95% C.L. limit of $\mathcal{B}(t \rightarrow Zq) < 10.4\%$ (expected limit: 6.8%), consistent with a 1σ upward fluctuation of the expected SM backgrounds.
[16] D. Sherman, Ph.D. Thesis, Harvard University (2007).
[17] A. L. Read, Nucl. Instrum. Methods A **425**, 357 (1999).
[18] D. Acosta *et al.*, Phys. Rev. Lett. **95**, 102002 (2005).